A STUDY OF THE GRAVITATIONAL WAVE PULSAR SIGNAL WITH ORBITAL AND SPINDOWN EFFECTS

S. R. Valluri*†, K. M. Rao*, P. Wiegert†, F. A. Chishtie*
email: valluri@uwo.ca, krao@uwo.ca, pwiegert@uwo.ca, fchishti@uwo.ca
Departments of *Applied Mathematics, †Physics & Astronomy, University of Western Ontario, London, Canada

Abstract

In this work we present analytic and numerical treatments of the gravitational wave signal from a pulsar which includes spindown. We consider phase corrections to a received monochromatic signal due to rotational and elliptical orbital motion of the Earth, as well as perturbations due to Jupiter and the Moon. We discuss the Fourier transform of such a signal, which is expressed in terms of well known special functions and lends itself to a tractable numerical analysis.

1 Introduction

The detection of gravitational waves (GW) from astrophysical sources is one of the outstanding problems in experimental gravitation today. Gravitational wave detectors like the LIGO, VIRGO, LISA, TAMA 300, GEO 600 and AIGO are opening a new window for the study of a great variety of nonlinear curvature phenomena. Detection of GW necessitates sufficiently long observation periods to attain adequate Signal to Noise ratio. The data analysis for continuous GW, for example from rapidly spinning neutron stars, is an important problem for ground based detectors that demands analytic, computational and experimental ingenuity.

In recent works [1, 2] we have implemented the Fourier transform (FT) of the Doppler shifted GW signal from a pulsar with the Plane Wave Expansion in Spherical Harmonics (PWESH). It turns out that the consequent analysis of the Fourier Transform (FT) of the GW signal from a pulsar has a very interesting and convenient development in terms of the resulting spherical Bessel, generalized hypergeometric, Gamma and Legendre functions. These works considered frequency modulation of a GW signal due to rotational and circular orbital motions of the detector on the Earth. In the present analysis, rotational and orbital eccentric motions of the Earth, as well as perturbations due to Jupiter and the Moon, and pulsar spindown are considered. This formalism has a nice analytic representation for the GW signal in terms of the special functions above. The signal can then be studied as a function of various parameters associated with the GW pulsar signal, as well as the orbital and rotational parameters of the Earth. A brief analysis considering the parameters for the Lunar and Jovian perturbations is included. A detailed analysis of the spindown and perturbation effects has been recently done [3]. The numerical analysis of this analytical expression for the signal offers a challenge for efficient and fast numerical and parallel computation.

In this work, we present a variation of a parametrized model of pulsar spindown discussed by Brady et al. [4] and Jaranowski et al. [5] for the GW frequency and the phase measured at the ground based detector that includes the spindown parameters. The various types of motion of the detector can be naturally incorporated into this parametrized spindown model. Effects of amplitude modulation (AM), though not considered in this paper, can also be incorporated into this formalism without great difficulty. We discuss the Fourier transform of the GW signal including the orbital and rotational corrections. In addition, a numerical study of the effects of the various detector motions on the phase of the GW signal and the dependence of the received signal on detector position and pulsar direction have been done. This might be relevant to GW detectors.

2 Gravitational Wave Signal with Spindown Corrections

Starting from a slightly modified form of the parameterization given by Brady and Creighton (2000)[4], we obtain the following expression for the phase of a gravitational wave signal [3] :

$$\phi(\tau,\lambda) = \pi f_0 \left[x + \tau_{min} \sum_{k=0}^{\infty} \frac{T_k(z)}{k+1} \left(\frac{x}{\tau_{min}} \right)^{k+1} \right] \tag{1}$$

The $T_k(z)$ $(-1 \leq T_k(z) \leq 1, \quad k \geq 0, \quad -1 \leq z \leq 1)$ are the Chebyshev polynomials, and $x = t + \frac{\vec{r}}{c} \cdot \hat{n}$, where $\vec{r}(t)$ is the position vector of the detector in the Solar System Barycentre (SSB) frame, and $\hat{n}$ is a unit vector in the direction of the pulsar. τ_{min} is the spindown age of the pulsar in years, and f_0 is the GW frequency without spindown. The series in this expression sums to

$$\sum_{k=0}^{\infty} \frac{T_k(z)}{k+1} \left(\frac{x}{\tau_{min}} \right)^{k+1} = -\frac{1}{2} \left[\ln \left(1 - 2 \left(\frac{x}{\tau_{min}} \right) z + \left(\frac{x}{\tau_{min}} \right)^2 \right) - 1 \right] \tag{2}$$

We have plotted this expression as a function of x for $\tau_{min} = 40$ and 1000 years for $z = -0.8, 0.7$ and 0.9 (see Appendix, Figure 1).

The GW signal is now given by

$$e^{i\phi(t,\lambda)} = e^{\frac{i\pi f_0 \tau_{min}}{2}} e^{i\pi f_0 x} \left[1 - \frac{i\pi f_0 \tau_{min}}{2} \left(-2 \left(\frac{x}{\tau_{min}} \right) z + \left(\frac{x}{\tau_{min}} \right)^2 \right) + ... \right]. \tag{3}$$

We have used the binomial expansion inside the square brackets. We define the Spindown Moment Integrals as follows:

$$\int_0^T e^{i\pi f_0\left(x+\frac{\tau_{min}}{2}\right)} \cdot e^{-i2\pi ft} \cdot \left(\frac{x+\frac{\tau_{min}}{2}}{\tau_{min}}\right)^k dt, \tag{4}$$

If we define

$$I_{generic} = \int_0^T e^{\left[i\pi f_0(x+\frac{\tau_{min}}{2})-i2\pi ft\right]} dt, \tag{5}$$

then the kth Spindown Moment Integral can be written as

$$\frac{1}{(i\pi\tau_{min})^k} \frac{\partial^k I_{generic}}{\partial f_0^k}. \tag{6}$$

Thus the Fourier transform of the signal can be written in terms of the partial derivatives with respect to f_0 of $I_{generic}$, which can be evaluated analytically.

3 Corrections to the Position Vector of the Detector

In this section we briefly outline the corrections to the position vector $\vec{r}(t)$ to account for the Keplerian ellipse, Earth's rotation, and the perturbations due to Jupiter and the Moon.

An expansion of the elliptical orbit of the Earth, to second-order in eccentricity, leads to the following expressions for the x and y components of $\vec{R}_{orb}$, the vector specifying the Earth's orbital position (the z component is 0) [6] :

$$x(t) = a\left(1-\frac{3}{8}e^2\right)\cos M + \frac{ae}{2}\cos 2M + \frac{3}{8}ae^2\cos 3M - \frac{3}{2}ae \tag{7-a}$$

$$y(t) = a\left(1-\frac{3}{8}e^2\right)\sin M + \frac{ae}{2}\sin 2M + \frac{3}{8}ae^2\sin 3M - \frac{1}{4}ae^2\sin M \tag{7-b}$$

(a = Sun-Earth distance, $M = \omega_{orb}t$, e = eccentricity of orbit.) If the radius of Jupiter's orbit is much greater than that of the Earth, we can consider the Sun, to a first approximation, as moving around the Sun-Jupiter (S-J) barycentre, and the Earth orbiting the Sun. Then, the perturbation $\vec{R}_J$ due to Jupiter is [3] :

$$\vec{R}_J = \left[R_J\left(\cos\left(\omega_J t\right)-1\right), R_J\sin\left(\omega_J t\right), 0\right] \tag{8}$$

where ω_J is the orbital angular frequency of Jupiter, and R_J is the distance of the Sun from S-J barycentre.

Similarly, the vector from the Earth-Moon barycentre to the Earth is:

$$\vec{R}_M = \begin{bmatrix} R_{EM}\left(\cos\left(\omega_M t\right) - 1\right) \\ R_{EM}\sin\left(\omega_M t\right) \\ 0 \end{bmatrix}. \tag{9}$$

Here ω_M is the Moon's sidereal orbital angular frequency, and R_{EM} is the distance from Earth to the Earth-Moon barycentre. Also, the vector specifying the detector's position due to the rotating Earth, $\vec{R}_{rot}$, is given by

$$\vec{R}_{rot} = \begin{bmatrix} R_E \sin\alpha\left(\cos\left(\omega_{rot} t\right) - 1\right) \\ R_E \sin\alpha \sin\left(\omega_{rot} t\right)\cos\varepsilon \\ R_E \sin\alpha \sin\left(\left(\omega_{rot} t\right)\sin\varepsilon\right. \end{bmatrix}, \tag{10}$$

where R_E = Earth's radius, α = detector co-latitude, ε = angular tilt of Earth's axis, and ω_{rot} = Earth's sidereal rotational angular frequency. The position of the detector is now given in the form:

$$\vec{r}(t) = \vec{R}_{orb}(t) + \vec{R}_{rot}(t) + \vec{R}_J(t) + \vec{R}_M(t) \tag{11}$$

4 Contributions of Perturbations to the Phase of the GW Signal

The contribution of a perturbation to the phase of the GW signal (in radians) is given by $\phi(t) = 2\pi f_0 \frac{\vec{r}_i(t)\cdot\hat{n}}{c}$, where $\vec{r}_i(t)$ is the contributing vector for the perturbation [2]. We have plotted the phase contributions for the Earth's circular and elliptical orbital and rotational perturbations, as well as contributions from the Jovian and Lunar perturbations, as functions of θ (the angle of the pulsar from the orbital plane normal) and ϕ (the angle of the pulsar from the x-axis in the orbital plane), for $t = 6$ lunar months (6×29.5 d), $\alpha = \frac{\pi}{2}$ and $f_0 = 1$ kHz (see Appendix, Figure 2.) In each plot, the maximum phase shift occurs near $\theta = \frac{\pi}{2}$ (when the pulsar direction is in Earth's orbital plane). The ϕ-value at the maximum is more variable. The approximate maximum phase shifts for the above perturbations are, respectively, 6.3×10^6, 3.2×10^6, 1.8×10^2, 2.6×10^4 and 1.2×10^2 radians. For comparison, the phase of the signal in this time period without Doppler shifts ($2\pi f_0 t$) is 9.6×10^{10} radians.

We have also plotted the positional errors from using the circular approximation versus those of equation 7, for a 1 kHz gravitational wave (see Appendix, Figure 3). Four orders of magnitude are gained, a substantial reduction in the error. In addition, we see that the phase error can be quite large if we ignore the effects of Jupiter and the Moon over long integration times.

5 The FT of the Perturbation-Corrected GW Pulsar Signal

In Valluri et al. (2005) [3], we arrive at an analytic expression for the Fourier transform of a GW signal, considering the perturbations above:

$$\widetilde{h}(f) = \sum_{r=-\infty}^{\infty}\sum_{s=-\infty}^{\infty}\sum_{N=-\infty}^{\infty}\sum_{n=-\infty}^{\infty}\sum_{l=0}^{\infty}\sum_{m=-l}^{l}\psi_0\psi_1\psi_2\psi_3\psi_4\psi_5\psi_6 \tag{12}$$

where

$$\psi_0(r,s,N,n,l,m,\alpha,\theta,\phi) = 4\pi i^{r+s+N+l}Y_{lm}(\theta,\phi)N_{lm}P_l^m(\cos\alpha)e^{-i(r+s+N)\phi}$$

$$\psi_1(n,\theta,\phi,f_0) = T_{Er}\sqrt{\tfrac{\pi}{2}}e^{-i\frac{2\pi f_0 a}{c}\sin\theta\cos\phi - in\phi}i^n J_n\left(\tfrac{2\pi f_0}{c}a\sin\theta\left(1-\tfrac{3}{8}e^2\right)\right)$$

$$\psi_2(l,n,m,r,s,N,f_0,\omega) = \left\{\tfrac{1-e^{i\pi(l-B_T)R}}{1-e^{i\pi(l-B_T)}}\right\}2e^{-iB_T\frac{\pi}{2}}\tfrac{1}{2^{2l+1}}$$

$$\psi_3(k,l,m,n,r,s,N,f_0,\omega) = k^{l+\frac{1}{2}}\tfrac{\Gamma(l+1)}{\Gamma\left(l+\frac{3}{2}\right)\Gamma\left(\frac{l+B_T+2}{2}\right)\Gamma\left(\frac{l-B_T+2}{2}\right)}$$

$$\psi_4(r,s,N,\theta,f_0) = J_r\left(\tfrac{2\pi f_0}{2c}ae\sin\theta\right)J_s\left(\tfrac{2\pi f_0}{c}R_J\sin\theta\right)J_N\left(\tfrac{2\pi f_0}{c}R_{EM}\sin\theta\right)$$

$$\psi_5(\theta,\phi,f_0) = \exp\left[-\tfrac{i2\pi f_o}{c}\sin\theta\cos\phi\left(\tfrac{3}{2}ae+R_J+R_{EM}\right)\right]$$

$$\psi_6(k,l,m,n,r,s,N,f_0,\omega) =_1 F_3\left(l+1; l+\tfrac{3}{2}, \tfrac{l+B_T+2}{2}, \tfrac{l-B_T+2}{2}; \tfrac{-k^2}{16}\right)$$

Here c is the speed of light, and $\omega_0 = 2\pi f_0$. Also,
$B_T = 2\left(\frac{\omega-\omega_0}{\omega_{rot}} + \frac{m}{2} + \frac{n}{2}\frac{\omega_{orb}}{\omega_{rot}} + \frac{r}{2}\frac{2\omega_{orb}}{\omega_{rot}} + \frac{s}{2}\frac{\omega_J}{\omega_{rot}} + \frac{N}{2}\frac{\omega_M}{\omega_{rot}}\right)$ and $k = \frac{4\pi f_0 R_E\sin(\alpha)}{c}$.

Feynman has thoroughly discussed the diffraction pattern due to the factor in the curly brackets in the expression for ψ_2 which gives the resultant amplitude due to R equal oscillators ($R = 365$ in our case) [7]. This factor is analogous to the expression for the scattering amplitude of an electron in a crystal lattice.

The intensity of the signal, $\left|\tilde{h}(f)\right|^2$, can be expressed in analytic form from Equation 12. A detailed numerical analysis of this expression for the variety of parameters, which can take huge values (> 50000), present in the GW signal is a challenge for high performance parallel computation [8].

6 Conclusions

We have presented in this paper the rudiments of a simple analysis for spindown for sources of continuous GW. For the more computationally intensive search over all sky positions and spindown parameters, it is important to be able to calculate the smallest number of independent parameter values which must be sampled in order to cover the entire space of signals. The PWESH improves

the numerical accuracy and convergence of analytic FT's, spindown corrections associated with the GW signal, and also enables the estimation of parameters and distributions relevant to GW Data Analysis. It has also found many important applications, for example in the study of the multipole moments in the Cosmic Microwave Background Anisotropies [9]. The proper blend of analytic and numerical integration for accurate GW data analysis remains an interesting question to be explored further.

7 Acknowledgments

We are deeply grateful to SHARCNET (Shared Hierarchical Academic Research Cluster Network) and NSERC for grant support. We are also greatly indebted to Drs. Nico Temme (CWI, Amsterdam), Martin Houde (UWO), James Hilton(Astronomical Applications Dept., US Naval Research Lab) and Manuel Gil (UWO) for valuable suggestions.

References

[1] K. Jotania, S.R. Valluri and S.V. Dhurandhar, Astron.Astrophys. **306**:317,1996.

[2] S.R. Valluri, F.A. Chishtie, et al. Class.Quant.Grav.**19**:1327-1334,2002, Erratum-ibid.19:4227-4228,2002.

[3] Valluri S. R., Chishtie F. A. and Vajda A. Submitted to Classical and Quantum Gravity, July 2005.

[4] Brady P. R. et al., Phys Rev. D, **61**, 082001, 2000; **57**, 2101, 1998.

[5] Jaranowski, P. et al., A. Phys.Rev. D **59**, 63003, 1999; **61**, 62001, 2000; **58**, 63001, 1998.

[6] Murray C. D. and Dermott, S. F. "Solar System Dynamics", Cambridge University Press, Cambridge, 1999.

[7] The Feynman Lectures on Physics, (Addison Wesley, Menlo Park, CA, 1975.

[8] Chishtie, F.A., Valluri S.R., Rao K.M., et al., IEEE Computer Society Press, Proc. 19th Annual Symposium, High Performance Computing Systems & Applications. (HPCS 2005), Guelph, Ont., Canada.

[9] Peacock John A. Cosmological Physics, Cambridge University Press, Cambridge, 1999.

8 Appendix

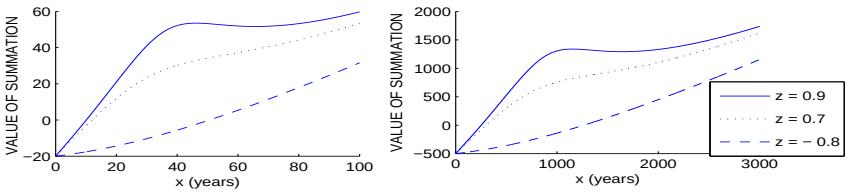

Figure 1: Plot of summation as a function of x for $\tau_{min} = 40$ years (left) and $\tau_{min} = 1000$ years (right) for different z values.

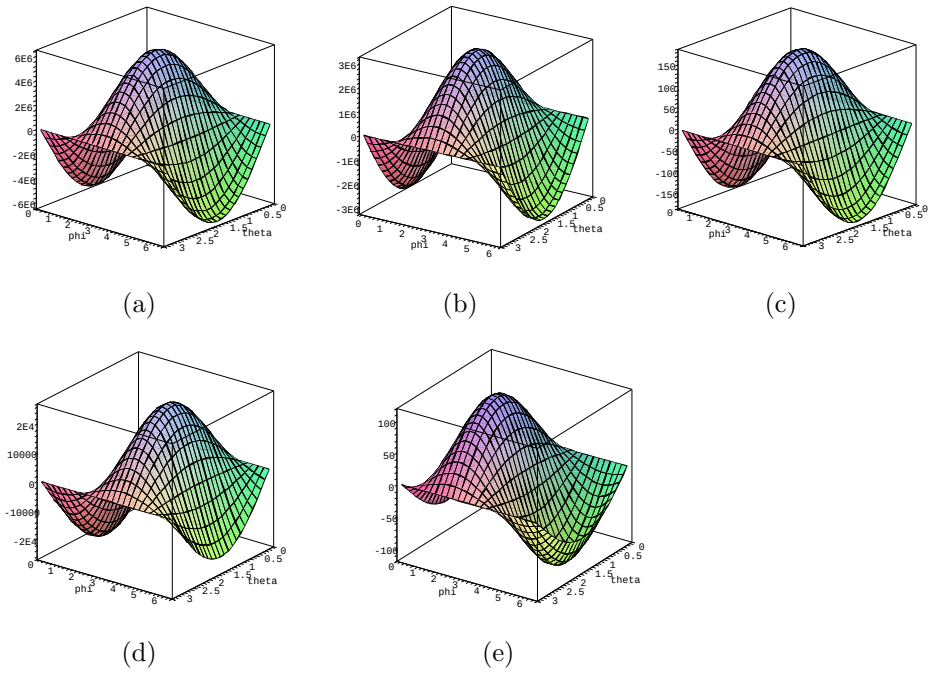

(a) (b) (c)

(d) (e)

Figure 2: Plot of phase shift due to (a) circular orbit, (b) elliptical orbit, (c) Earth's rotation, (d) Jupiter, and (e) the Moon, as a function of θ and ϕ.

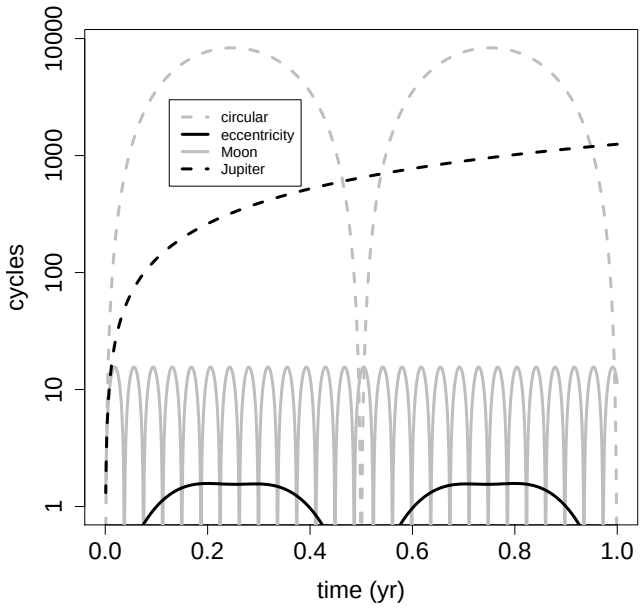

Figure 3: The difference between the Earth's position as computed by a circular approximation versus a Keplerian one, measured in cycles of a 1 kHz gravitational wave over the course of one year (dashed grey line). The (much reduced) difference when equation 7 is used is shown as a solid black line. Approximate contributions to the motion of the Earth due to the Moon and Jupiter are shown for comparison.